

# Minimum Time Orbit Raising of Geostationary Spacecraft by Optimizing Feedback Gain of Steering-law

By Kenji KITAMURA<sup>1)</sup>, Katsuhiko YAMADA<sup>2)</sup> and Takeya SHIMA<sup>1)</sup>

<sup>1)</sup> Advanced Technology R&D Center, Mitsubishi Electric Corporation, Amagasaki, Japan

<sup>2)</sup> Graduate School of Engineering, Osaka University, Osaka, Japan

(Received June 21st, 2017)

In this study, the minimum time orbit raising problem of geostationary spacecraft by the low propulsion thrusters is considered. This problem is equivalent to how to determine an appropriate thrust direction during the orbit raising. This study proposes a closed loop thruster steering-law that determines the thrust direction based on the optimal feedback gains and the control errors of each orbital element. The feedback gains of the steering-law are assumed to be the functions of orbital elements, and they are optimized by the meta-heuristic method such as a particle swarm optimization. As an independent variable for expressing the gains, the orbital semi-major axis, eccentricity, and inclination are considered. Numerical simulations show that whichever orbital element of these is selected for the independent variable, the same performances are obtained. This guarantees that regardless of the initial orbital elements, by selecting the independent variable appropriately, the minimum time orbit transfer problem can always be solved by the proposed method.

**Key Words:** Orbit Raising, Geostationary Orbit, Low Propulsion Thruster, Optimal Control

## Nomenclature

$a$	: semi-major axis
$e$	: eccentricity
$i$	: inclination
$\omega$	: argument of perigee
$\Omega$	: right ascension of ascending node
$\nu$	: true anomaly
$E$	: eccentric anomaly
$p$	: semi-latus rectum(= $a(1 - e^2)$ )
$h$	: orbit angular momentum(= $\sqrt{\mu p}$ )
$n$	: mean angular motion
$L$	: true longitude(= $\Omega + \omega + \nu$ )
$(e_x, e_y)$	: eccentricity vector
$(i_x, i_y)$	: inclination vector
$x$	: $6 \times 1$ vector which consists of slow equinoctial elements and mass (= $[a \ e_x \ e_y \ i_x \ i_y \ m]^T$ )
$T$	: orbital period(= $2\pi/n$ )
$r$	: distance from center of Earth to spacecraft
$R_e$	: equatorial radius of Earth
$\mu$	: gravitational constant of Earth
$g$	: gravitational acceleration of Earth at sea level
$t$	: time
$T$	: orbital period(= $2\pi/n$ )
$I_{sp}$	: specific impulse of thruster
$F_T$	: magnitude of thruster force
$m$	: spacecraft mass
$\alpha$	: in-plane thruster steering angle
$\beta$	: out-of-plane thruster steering angle

## Subscripts

0	: initial
$f$	: final
$r$	: radial direction in LVLH coordinates
$\theta$	: transversal direction in LVLH coordinates
$h$	: normal direction in LVLH coordinates

## 1. Introduction

In recent years, a low propulsion thruster such as an ion-thruster or a hall thruster is becoming a hopeful propulsion system for a spacecraft transferring from a low earth orbit (LEO), a geostationary transfer orbit (GTO), or a supersynchronous orbit (SSTO) to a geostationary orbit (GEO).<sup>1-3)</sup> Conventionally, a geostationary spacecraft is just putted in the GTO by a launcher and in order to complete the orbit transfer, the spacecraft employs an on-board high chemical propulsion thruster called apogee kick motor at the apogee of GTO so that the orbit semi-major axis, eccentricity, and inclination correspond with those of GEO.<sup>4)</sup> Although GEO insertion by the chemical propulsion thruster completes in a short period of time (generally less than one week, including initial check-out operation time), a low specific impulse of the thruster results in much fuel consumption (almost half of the wet mass is occupied by the fuel). In order to overcome this disadvantage, a spiral orbit raising by the low propulsion electric thruster, which has almost ten times larger specific impulse than the chemical propulsion, is getting a lot of attention as an alternative transfer orbit<sup>5)</sup>. In the case of the spiral orbit raising, it takes several months to complete the orbit transfer but it can save a lot of fuel.

In the past, a lot of works that aim to optimize the orbit

transfer with the low propulsion have been conducted. Sackett et al.<sup>6)</sup> utilized the averaging method and solved the problem by the classical indirect optimization. Kluever et al.<sup>7,13)</sup> solved the optimal control problem by a direct optimization approach where the costate variables or the weighting variables are the optimization variables of the nonlinear programming problem. Graham et al.<sup>10)</sup> posed the minimum-time trajectory optimization as a multiple-phase optimal control problem and solved it by a pseud-spectral method. Ruggiero et al.<sup>11)</sup> proposed a closed loop steering-law which determines the thrust direction based on the difference between the current orbital elements and the target ones.

In this study, the minimum time orbit transfer problem by the low propulsion thrusters is considered. This problem is equivalent to how to determine the appropriate thrust direction during the orbit raising. In order to obtain the optimal direction, the closed loop thruster steering-law given by Ref. 11) is improved in this paper. In detail, the feedback gains for the steering-law are introduced to obtain the optimal thruster direction. The feedback gains are expressed as the functions of a monotonically increasing or decreasing orbital element, and they are optimized by the meta-heuristic method such as a particle swarm optimization. As an independent variable for expressing the gains, the orbital semi-major axis, eccentricity, or inclination is chosen. Numerical simulations show that whichever orbital element of these is selected for the independent variable, almost the same performances are obtained.

## 2. Dynamics of Osculating and Mean Orbital Elements

In this paper, the following equinoctial orbital elements  $(a, e_x, e_y, i_x, i_y, L)$  which are defined by Eqs. (1)-(4) are utilized for describing the orbital motion.<sup>14)</sup>

$$e_x = e \cos(\Omega + \omega) \quad (1)$$

$$e_y = e \sin(\Omega + \omega) \quad (2)$$

$$i_x = \tan(i/2) \cos \Omega \quad (3)$$

$$i_y = \tan(i/2) \sin \Omega \quad (4)$$

$$L = \Omega + \omega + \nu$$

where  $(e_x, e_y)$ ,  $(i_x, i_y)$ , and  $L$  are called an eccentricity vector, an inclination vector, and true longitude, respectively.

### 2.1. Dynamics of osculating equinoctial elements

The equinoctial elements have the merit of singularity-freeness, and these equations of motion are written as follows:

$$\frac{da}{dt} = \frac{2}{n\sqrt{1-e^2}} \left( e \sin \nu u_r + \frac{p}{r} u_\theta \right) \quad (5)$$

$$\frac{de_x}{dt} = q \sin L u_r + \frac{q}{w} [(w+1) \cos L + e_x] u_\theta - \frac{qz}{w} e_y u_h \quad (6)$$

$$\frac{de_y}{dt} = -q \cos L u_r + \frac{q}{w} [(w+1) \sin L + e_y] u_\theta + \frac{qz}{w} e_x u_h \quad (7)$$

$$\frac{di_x}{dt} = \frac{qs^2}{2w} \cos L u_h \quad (8)$$

$$\frac{di_y}{dt} = \frac{qs^2}{2w} \sin L u_h \quad (9)$$

$$\frac{dL}{dt} = \sqrt{\mu p} \left( \frac{w}{p} \right)^2 + \frac{qz}{w} u_h \quad (10)$$

where  $q, w, z$ , and  $s$  are defined as follows:

$$q = \sqrt{p/\mu} \quad (11)$$

$$w = 1 + e_x \cos L + e_y \sin L \quad (12)$$

$$z = i_x \sin L - i_y \cos L \quad (13)$$

$$s^2 = 1 + i_x^2 + i_y^2 \quad (14)$$

In Eqs. (5)-(10),  $u_r, u_\theta$ , and  $u_h$  are the perturbing acceleration on spacecraft expressed in a local vertical local horizontal (LVLH) coordinate, whose  $r$  axis points to the spacecraft from the center of the Earth,  $h$  axis is perpendicular to the orbital plane, and  $\theta$  axis is chosen to complete the right hand system. The spacecraft mass flow rate due to the thruster operation is expressed as follows:

$$\frac{dm}{dt} = -\frac{F_T}{gI_{sp}} \quad (15)$$

### 2.1. Dynamics of mean equinoctial elements

Generally, an orbit transfer by a low-propulsion thruster requires several months, and it takes rather long time to numerically integrate the osculating equinoctial elements. This can lead to the long convergence time in the numerical optimization process where the iterative integration is required. In order to reduce the integration time, we utilize the following averaged dynamics of equinoctial elements as was done by Kluever<sup>7)</sup> and Utashima<sup>8)</sup>:

$$\frac{d\bar{x}}{dt} = \frac{1}{T} \int_{E_b}^{E_e} \frac{dx}{dt} dt = \frac{1}{2\pi} \int_{E_b}^{E_e} \frac{dx}{dt} (1 - e \cos E) dE \quad (16)$$

where  $\bar{x}$  is a vector composed of slow-variables of the equinoctial elements and spacecraft mass. In Eq. (16), the relation of  $dE/dt = n/(1 - e \cos E)$  is used. The eccentric anomaly  $E_b$  and  $E_e$  represent the beginning and ending of the thruster arc in one orbit revolution, respectively. In the Earth eclipse (shadow), it is assumed that the power cannot be generated and that the thruster is turned off. Therefore,  $E_b$  and  $E_e$  correspond to the exit and entry point of Earth eclipse in one orbit revolution, respectively. If there are no coasting arc,  $E_b$  and  $E_e$  can be set to 0 and  $2\pi$ , respectively. The model of the Earth eclipse is briefly described in the next section.

### 2.3. Model of Earth eclipse

The earth shadow related to the satellite orbiting the Earth is composed of two regions. One is a penumbra and the other is an umbra. In the penumbra, the sun light is partially obscured by the Earth, while in the umbra, the light is completely blocked. In this paper,  $E_b$  and  $E_e$  are determined based on the exit and entry point of penumbra, respectively, by using a manner similar to Ref. 9).

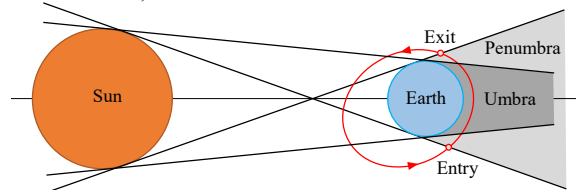


Fig. 1. The geometry of Earth shadow.

### 3. Steering-law

In this section, we describe the proposed thruster steering-law for the low-thrust orbit transfer. This is the improvement of the one studied by Ruggiero<sup>11)</sup>. We first briefly review the conventional method, and then describe the improved steering-law of this study.

#### 3.1. Conventional steering law

In this study, we assume that the thruster force  $F_T$  keeps a constant value, and that the thruster direction is controlled. By introducing a pitch angle  $\alpha$  and a yaw angle  $\beta$  (Fig. 2), the thruster force vector can be expressed in the LVLH coordinate as follows:

$$u_r = a_T \sin \alpha \cos \beta \quad (17)$$

$$u_\theta = a_T \cos \alpha \cos \beta \quad (18)$$

$$u_h = a_T \sin \beta \quad (19)$$

where  $a_T$  is a thruster acceleration, defined by  $F_T/m$ . Substituting Eqs. (17)-(19) into the gauss-planetary equations of the semi-major axis, eccentricity, and inclination, following equations are obtained:

$$\frac{da}{dt} = \frac{2a^2}{h} \cos \beta \left( e \sin v \sin \alpha + \frac{p}{r} \cos \alpha \right) a_T \quad (20)$$

$$\frac{de}{dt} = \frac{1}{h} \cos \beta \left[ p \sin v \sin \alpha + ((p+r) \cos v + re) \cos \alpha \right] a_T \quad (21)$$

$$\frac{di}{dt} = \frac{r}{h} \cos(\omega + v) \sin \beta a_T \quad (22)$$

By setting the first derivative of Eqs. (20)-(22) with respect to  $\alpha$  and  $\beta$  equal to zero and solving them, the optimal pitch and yaw angles to maximize the rate of change of these three orbital elements are obtained as shown in Table 1.

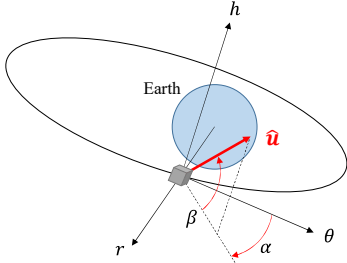


Fig. 2. Geometry of LVLH coordinates and thruster direction.

Table 1. Optimal steering angle for maximum rate of change of semi-major axis, eccentricity, and inclination

	Pitch angle	Yaw angle
semi-major axis	$\tan^{-1} \left( \frac{e \sin v}{1 + e \cos v} \right)$	0
eccentricity	$\tan^{-1} \left( \frac{\sin v}{\cos v + \cos E} \right)$	0
inclination	any	$\text{sign}(\cos(\omega + v)) \frac{\pi}{2}$

Let us define the optimal pitch and yaw angle for changing semi-major axis, eccentricity, and inclination as  $\alpha_j^*, \beta_j^*$  ( $j = a, e, i$ ). The associating optimal thrust direction  $\hat{\mathbf{u}}_j^*$  ( $j = a, e, i$ ) is expressed as follows:

$$\hat{\mathbf{u}}_j^* = [\sin \alpha_j^* \cos \beta_j^* \quad \cos \alpha_j^* \cos \beta_j^* \quad \sin \beta_j^*]^T \quad (23)$$

Ref. 11) proposed calculating the thrusting vector as a weighted linear sum of  $\hat{\mathbf{u}}_a^*$ ,  $\hat{\mathbf{u}}_e^*$ , and  $\hat{\mathbf{u}}_i^*$  where the weights are determined by the difference between the osculating value of the specific orbital element and the target one of the same element. This calculation is given as follows:

$$\hat{\mathbf{u}} = \frac{\mathbf{u}}{|\mathbf{u}|} \quad (24)$$

$$\mathbf{u} = \left( \frac{a_f - a}{a_f - a_0} \right) \hat{\mathbf{u}}_a^* + \left( \frac{e_f - e}{e_f - e_0} \right) \hat{\mathbf{u}}_e^* + \left( \frac{i_f - i}{i_f - i_0} \right) \hat{\mathbf{u}}_i^* \quad (25)$$

where subscript 0 and  $f$  represent the initial and final (target) value of each orbital element, respectively.

#### 3.2. Proposed steering-law

The conventional method in the previous section introduces self-adaptive weights and blends each optimal direction  $\hat{\mathbf{u}}_j^*$  in accordance with the weights. By using this steering-law, it can be expected that the all orbital elements will converge to the desired values with the lapse of time. However, these self-adaptive weights are not necessarily optimal, and we propose to improve the steering-law as follows:

$$\hat{\mathbf{u}} = \frac{\mathbf{u}}{|\mathbf{u}|}, \quad \mathbf{u} = w_a \hat{\mathbf{u}}_a^* + w_e \hat{\mathbf{u}}_e^* + w_i \hat{\mathbf{u}}_i^* \quad (26)$$

where the improved weights  $w_a, w_e$ , and  $w_i$  are given as:

$$w_a = K_a(\gamma) \frac{a_f - a}{|a_f - a_0|} \quad (27)$$

$$w_e = K_e(\gamma) \frac{e_f - e}{|e_f - e_0|} \quad (28)$$

$$w_i = K_i(\gamma) \frac{i_f - i}{|i_f - i_0|} \cdot \cos(\omega + v) \quad (29)$$

In the above equations,  $K_a(\gamma), K_e(\gamma)$ , and  $K_i(\gamma)$  are the feedback gains of the each self-adaptive weight, and they are the functions of monotonically increasing or decreasing orbital element  $\gamma$ . In the case of the coplanar GTO to GEO transfer, the semi-major axis or eccentricity can be chosen to be  $\gamma$ , while if the initial semi-major axis is equal to that of GEO (the case of SSTO to GEO), the eccentricity or inclination can be chosen, for example. Because the relative values of the weights are important, one of the gains can be set one (ex.  $B_e(\gamma) = 1$  in the case of GTO to GEO). In the following section, the method to obtain the optimal gains  $K_a(\gamma), K_e(\gamma)$ , and  $K_i(\gamma)$  is described in detail. Also, we explain the reason why monotonically increasing orbital element  $\gamma$  is used as an independent variable instead of time.

## 4. Optimization of Feedback Gain for Minimum-time Orbit transfer

In this section, we describe the method to calculate the optimal feedback gains for the minimum-time orbit transfer. In section 4.1., the minimum-time transfer problem (an objective function and search variables) are defined, and in the succeeding section, the way of solving the optimization problem is described.

### 4.1. Problem of minimum-time transfer to GEO

#### 4.1.1. Objective function

In order to complete the orbit transfer to GEO, all of the semi-major axis, eccentricity, and inclination have to correspond to those of GEO. Because the steering-law given by

Eqs. (26)-(29) does not assure that the three orbital elements simultaneously achieve target values, a time when each orbital element gets its target value should be explicitly distinguished from each other as  $t_{fa}$ ,  $t_{fe}$ , and  $t_{fi}$  (Fig. 3). Therefore, the objective function of the minimum-time transfer to GEO is defined by the following min-max problem:

$$\min. J = \max(t_{fa}, t_{fe}, t_{fi}) \quad (30)$$

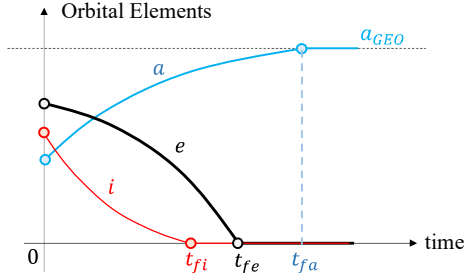


Fig. 3. Conceptual diagram of the time difference of each orbital element achieving the target value.

#### 4.1.2. Optimization variable

Our goal is to obtain the optimal feedback gains  $K_a(\gamma)$ ,  $K_e(\gamma)$ , and  $K_i(\gamma)$  which minimize the objective function  $J$ . In order to achieve this, the feedback gains are discretized within the interval of  $[\gamma_0, \gamma_f]$ , and the nodal values are optimized.

By dividing the interval  $[\gamma_0, \gamma_f]$  into  $(N - 1)$  segments, the  $k$ -th node  $\gamma_k$  is given as follows ( $k = 0, \dots, N - 1$ ):

$$\gamma_k = \gamma_0 + \frac{k}{N-1}(\gamma_f - \gamma_0) \quad (31)$$

The arbitrary  $K_j(\gamma)$  between the nodes  $\gamma_k$  and  $\gamma_{k+1}$  is calculated by a linear interpolation of  $K_j(\gamma_k)$  and  $K_j(\gamma_{k+1})$  as follows ( $k = 0, \dots, N - 2$ ):

$$K_j(\gamma) = K_j(\gamma_k) + \frac{K_j(\gamma_{k+1}) - K_j(\gamma_k)}{\gamma_{k+1} - \gamma_k}(\gamma - \gamma_k) \quad (32)$$

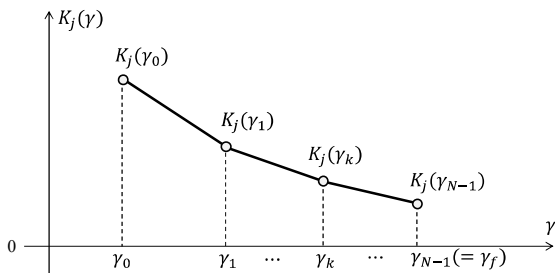


Fig. 4. Discretization of feedback gain through  $\gamma$ .

Because  $\gamma_0$  and  $\gamma_f$  are given from the initial and final condition, the objective is to obtain the optimal nodal values  $K_j(\gamma_k)$  ( $j = a, e, i; k = 0, \dots, N - 1$ ) which minimize the objective function. If all of the nodal values are given, the thruster vector can be calculated from Eq. (26) and it is possible to propagate the orbital elements forward. The Propagation ends when all of the semi-major axis, eccentricity, and inclination get to the target values. Therefore, the time  $t_{fa}$ ,  $t_{fe}$ , and  $t_{fi}$ , as well as objective function  $J$  are easily obtained by just forward propagating the equation of motion.

Note that if the time is chosen to be an independent variable instead of  $\gamma$ , it is impossible to propagate the orbital elements. This is because the final time  $t_f$  is an unknown variable, and the feedback gain cannot be interpolated in the time domain.

#### 4.2. Solving optimal feedback gain by particle swarm optimization

The objective function given in Eq. (29) is a min-max function and it is difficult to define its gradient. This means that the gradient-based solving methods for a nonlinear programming problem such as an interior-point method or a sequential quadratic programming method are not suitable for this min-max problem. In order to solve this problem and to get the optimal nodal values, we propose to utilize the particle swarm optimization (PSO). PSO is a meta-heuristic optimization method invented by Kennedy and Eberhart<sup>12)</sup>, and does not require any gradient information. In the following, the PSO algorithm used in this paper is briefly described.

Let us assume that we have total  $M$  particles in the search space, and that the position of the  $m$ -th particle at the  $k$ -th generation is defined as  $\mathbf{y}_k^m$ , where  $\mathbf{y}$  denotes a vector composed of all of the optimization variables (nodal values of feedback gains). The personal best of the  $m$ -th particle at the  $k$ -th generation  $\mathbf{p}_k^m$  is defined as follows:

$$\mathbf{p}_k^m = \mathbf{y}_j^{m*}, \quad j^* = \operatorname{argmin}_{0 \leq j \leq k} f(\mathbf{y}_j^m) \quad (33)$$

where  $f(\mathbf{y}_j^m)$  represents evaluating the objective function at  $\mathbf{y}_j^m$ . Furthermore, the optimal particle at the  $k$ -th generation is defined as the global best  $\mathbf{g}_k$  as follows:

$$\mathbf{g}_k = \mathbf{y}_k^{m*}, \quad m^* = \operatorname{argmin}_{1 \leq m \leq M} f(\mathbf{y}_k^m) \quad (34)$$

By using the personal best and global best, the state of each particle at the  $(k + 1)$ -th generation is updated as follows:

$$\mathbf{v}_{k+1}^m = w_k \mathbf{v}_k^m + c_p P_k(\mathbf{p}_k^m - \mathbf{y}_k^m) + c_g G_k(\mathbf{g}_k - \mathbf{y}_k^m) \quad (35)$$

$$\mathbf{y}_{k+1}^m = \mathbf{y}_k^m + \mathbf{v}_{k+1}^m \quad (36)$$

where  $w_k$  is a positive parameter that represents the inertia of particles at the  $k$ -th generation. The parameters  $c_p$  and  $c_g$  determine how strongly each particle is attracted to the particle best and global best, respectively. The parameter  $P_k$  and  $G_k$  are  $M \times M$  diagonal matrices, whose components are randomly sampled from a interval  $[0, 1]$  at every generations. In this paper, it is assumed that the attracting factor  $c_p$  and  $c_g$  are constant for the every generation, and that the inertia parameter  $w_k$  monotonically decreases with the lapse of generation. By defining the number of final generation as  $G$ ,  $w_k$  is given as follows ( $k = 0, \dots, G$ ):

$$w_k = w_0 + \frac{k}{G}(w_G - w_0) \quad (37)$$

where  $w_0$  and  $w_G$  represent the inertia parameter at the initial and final generation, respectively. By gradually decreasing the inertia parameter, each particle can independently move in the search space at the beginning, and can easily converge to the global best at the end.

## 5. Numerical Examples

In this section, numerical examples of the proposed optimization method are presented. By assuming GTO parameters, the initial orbital elements and mass are set as follows:

$$a_0 = 24,771\text{km}, \quad e_0 = 0.702, \quad i_0 = 28.5^\circ, \\ \Omega_0 = 30^\circ, \quad \omega_0 = 0^\circ, \quad m_0 = 1500\text{kg}$$

The thruster force  $F_T$  and specific impulse  $I_{sp}$  are set as 623.2mN and 1800sec, respectively. This  $a_0$  and  $e_0$  represent a perigee altitude of 1000km and an apogee of 35,786km. The target orbital elements of GEO are  $a_f = 42,164\text{km}$ ,  $e_f = 0$ , and  $i_f = 0^\circ$ . The departure date is set at 21st June, 2017. As for the independent variable  $\gamma$ , the following three cases are considered:

case1	case2	case3
semi-major axis	eccentricity	inclination

The number of the nodes are set at three for each case. With respect to the parameters of PSO, the following values are chosen: the particle population  $M = 75$ , the initial inertia  $w_0 = 0.9$ , the final inertia  $w_G = 0.4$ , the final generation  $G = 100$ , the particle best attraction  $c_p = 0.5$ , and the global best attraction  $c_g = 1.25$ . In this numerical examples, no perturbations except thruster force are considered and in the evaluation of each particle's score, the averaged equation of motion Eq. (16) is utilized for accelerating the propagation speed of orbital elements.

The summary of the transfer time of three cases as well as the conventional method is shown in Table 3. In three cases,  $t_{fa}$ ,  $t_{fe}$ , and  $t_{fi}$  have almost the same values and the transfer time is about 70.3day. On the other hand, as for the result of the conventional method,  $t_{fa}$ ,  $t_{fe}$ , and  $t_{fi}$  are different from each other by several days and transfer time is 83.6day, which is about 13days longer than that of the proposed method.

Figures 6-8 compare the time histories of the osculating semi-major axis, eccentricity, and inclination obtained by the conventional and proposed steering-laws. Note that these results are obtained by numerically propagating the osculating orbital elements by the optimized feedback gains. These figures show that no matter which orbital element among  $a$ ,  $e$ , and  $i$  is chosen as an independent variable, almost the same histories of orbital elements are obtained.

Figure 8 shows the 3D view of the transfer orbit of case1 in the inertial coordinate. Figure 9 compares the transfer orbit of case1 with that of the conventional method. It is clear that the maximum apogee altitude of case1 is much higher than the conventional method. This means that the proposed method prioritizes increasing the semi-major axis than decreasing the eccentricity at the initial phase of the transfer, which is also indicated by Figs. 5 and 6.

Figures 10-12 show the feedback gains obtained as the function of the semi-major axis, eccentricity, and inclination, respectively. Because the relative value of the gains is important,  $K_e$  is set at one for all cases. Note that in Figs. 11

and 12, the horizontal axes are reversed for the comparison with Fig. 10. These figures show the same trend that  $K_a$  and  $K_i$  are decreasing with the lapse of time. Although the three cases have the different values of the feedback gains, they share the same transfer time. This implies that the shape of  $\gamma - K_j$  curve is rather important than the absolute value of  $K_j$

Table 3. Comparison of transfer time

	case1 ( $\gamma = a$ )	case2 ( $\gamma = e$ )	case3 ( $\gamma = i$ )	conventional
$t_{fa}$	68.7	69.6	69.8	73.0
$t_{fe}$	70.2	70.3	70.2	77.5
$t_{fi}$	69.9	70.3	70.2	83.6
$t_f$	70.2	70.3	70.2	83.6

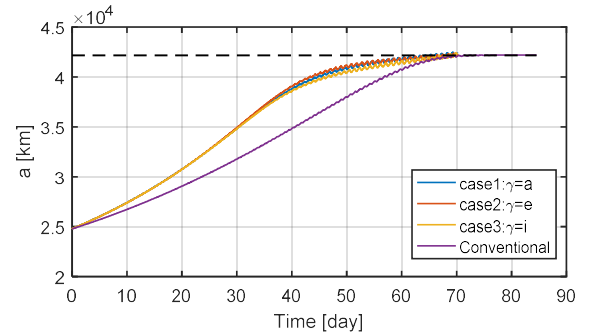


Fig. 5. Comparison of semi-major axis time history. The dashed line indicates the semi-major axis of GEO (42,164km)

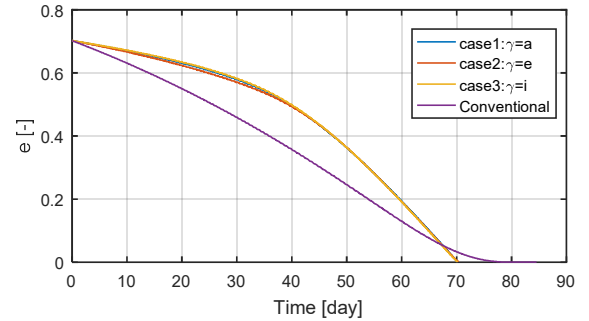


Fig. 6. Comparison of eccentricity time history

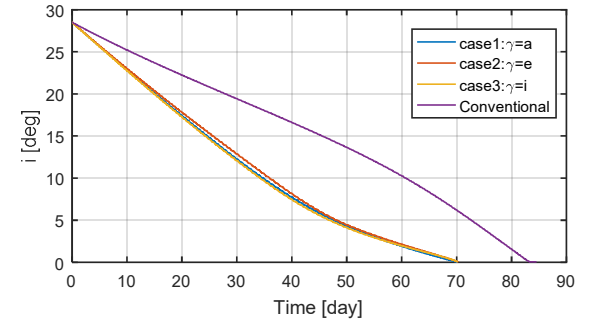


Fig. 7. Comparison of inclination time history

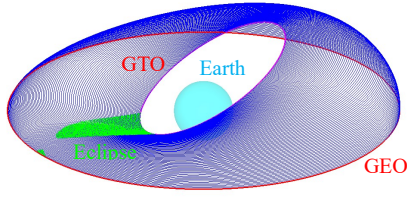


Fig. 8. 3D view of GTO to GEO transfer trajectory of obtained by proposed method (case1). A green area represents eclipse.

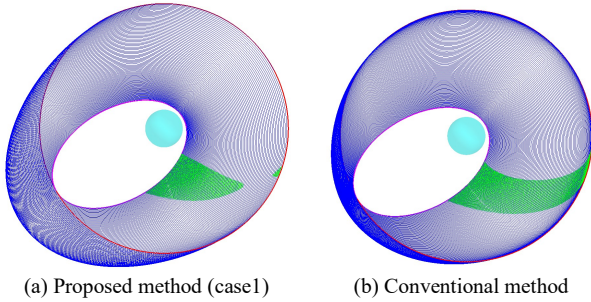


Fig. 9. Comparison of GTO to GEO transfer trajectory obtained by the proposed method (a) and the conventional one (b). A green area represents eclipse. The view point is above the Earth north-pole.

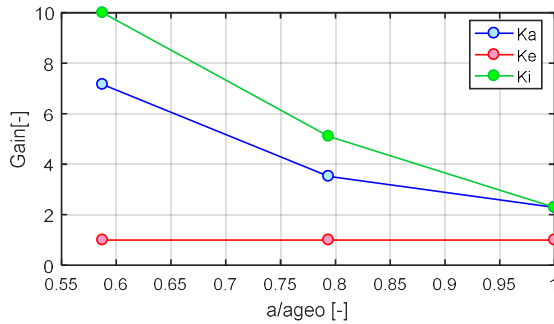


Fig. 10. Optimal gains as the functions of semi-major axis (case1)

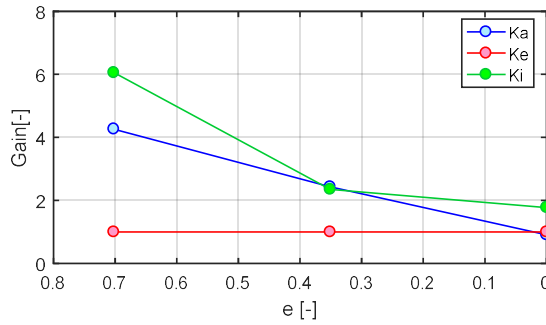


Fig. 11. Optimal gains as the functions of eccentricity (case2)

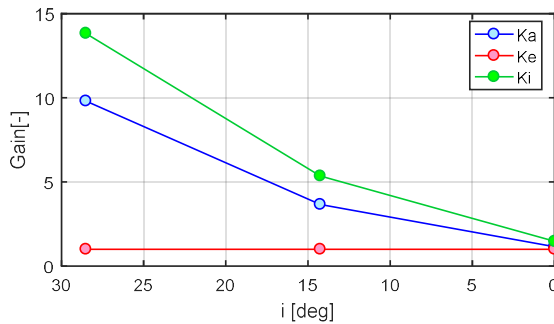


Fig. 12. Optimal gains as the functions of inclination (case3)

## 6. Conclusion

In this paper, we proposed a closed-loop thruster steering-law that determines the thrust direction based of the difference between the current orbital elements and the target ones. The feedback gains of the steering-law are assumed to be the functions of orbital elements, and they are optimized by a particle swarm optimization. In order to show the validity of the proposed method, some numerical simulations of the orbit transfer from GTO to GEO are conducted. The results disclosed that the proposed method can reduce the transfer time by 15% compared to the conventional steering-law, and that whichever orbital element that monotonically increase or decrease is selected for an independent variable, almost the same performances are obtained. This guarantees that regardless of the initial orbital elements, by selecting the independent variable appropriately, the minimum time orbit transfer problem can always be solved by the proposed method.

## References

- 1) Feuerborn, S. A., Neary, D. A., and Perkins, J. M.: Finding a way: Boeing's "All Electric Propulsion Satellite", 49th AIAA/ ASME/ SAE/ASEE Joint Propulsion Conference, San Jose, CA, AIAA 2013-4126, 2013.
- 2) Duchemin, O. B., Caratge, A., Cornu, N., Sannino J. M., Lassoudiere, F., and Lorand, A.: Ariane 5-ME and Electric Propulsion GEO Insertion Options, 47th AIAA/ ASME/ SAE/ ASEE Joint Propulsion Conference, San Diego, CA, AIAA 2011-6084, 2011.
- 3) Rezugina, E and Demaire, A.: All EP Platform Mission Design Challenges and Subsystem Design Opportunities, 33rd International Electric Propulsion Conference, Washington, USA, IEPC-2013-93, 2013.
- 4) Dalglish, D. I.: *An introduction to Satellite Communications*, IEE telecommunications series, IET, Stevenage, 1989, pp. 58-59.
- 5) Sanchez, M. M., and Pollard, J. E.: Spacecraft electric Propulsion An Overview, *J. Propulsion and Power*, **14** (1998), pp. 688-699.
- 6) Sackett, L. L., Malchow, H. L., and Edelbaum, T. N.: Solar Electric Geocentric Transfer with Attitude Constraints: Analysis, NASA CR-134927, 1975.
- 7) Kluever, C. A. and Oleson, S. R.: Direct Approach for Computing Near-Optimal Low-Thrust Earth-Orbit Transfers, *J. Spacecraft and Rockets*, **35** (1998), pp. 509-515.
- 8) Utashima, M.: Optimization of Orbital Transfer to Geostationary Earth Orbit by Solar Electric Propulsion, NASDA-TMR-020027, 2003 (in Japanese).
- 9) Neta, B. and Vallado, D.: On Satellite Umbra-Penumbra Entry and Exit Positions, *J. Astronomical Sciences*, **46** (1998), pp. 91-103.
- 10) Graham, K. F. and Rao, A. V.: Minimum-Time Trajectory Optimization of Low-Thrust Earth-Orbit Transfers with Eclipsing, *J. Spacecraft and Rockets*, **53** (2016), pp. 289-303.
- 11) Ruggiero, A and Pergola, P.: Low-thrust Maneuvers for the Efficient Correction of Orbital Elements, 32nd International Electric Propulsion Conference, Wiesbaden, Germany, IEPC-2011-102, 2011.
- 12) Kennedy, J. and Eberhart, R. C.: Particle Swarm Optimization, *Proc. IEEE International Conference on Neural Networks*, **4** (1995), pp. 1942-1948.
- 13) Conway, B. A. and Kluever, C. A.: *Spacecraft Trajectory Optimization*, Cambridge University Press, New York, 2010, pp. 113-137.
- 14) Broucke, R. A., and Cefola, P. J.: On the equinoctial orbit elements, *Celestial Mechanics*, **5** (1972), pp. 303-310.